Network of European Neuroscience Schools (NENS)

Stipends for Training Stays

Report

Douglas Asede

Recipient's email address: douglas.asede@cin.uni-tuebingen.de

Contact information of home institution supervisor: Dr. Ingrid Ehrich, Physiology of Learning and Memory, Hertie Institute for Clinical Brain Research & Centre for Integrative Neuroscience, Otfried-Müller Str 25 D-72076 Tübingen,
Germany.
ingrid.ehrlich@uni-tuebingen.de

Contact information of host institution supervisor: Prof. Francesco Ferraguti, Innsbruck Medical University, Pharmacological Department, Peter Myer Strasse 1a, 6020 Innsbruck, Austria.

Period of training stay: 18 May-30 June, 2012

Introduction

A large number of studies have shown that the amygdala is one of the key brain structures for acquisition and storage of fear memory (LeDoux, 2000, Maren et al., 2001). The amygdala consists of several anatomically and functionally distinct nuclei, including the lateral (LA) and basal (BA) nuclei (together referred to as the basolateral amygdala (BLA) and the central nuclei (CEA) ((Krettek and Price, 1978, Killcross et al., 1997). The lateral structures (BLA) are cortex-like, consisting of a majority of glutamatergic projection neurons and a minority of local GABAergic interneurons (McDonald, 1982). The medial structures (CEA) are striatum-like, with the vast majority of GABAergic neurons with medium spiny-type morphology (McDonald, 1982, Swanson and Petrovich, 1998).

The BLA is bounded laterally and medially by cortical fiber tracts referred to as external and intermediate capsule, respectively. Situated on these fiber bundles, are masses of clustered GABAergic neurons referred to as the intercalated cell clusters (ITCs) (Millhouse, 1986, Pare and Smith, 1993). Historically, they were divided into three major groups based on locations; the lateral paracapsular clusters (lpITC) located along the external capsule, the medial paracapsular clusters (mpITC), located along the intermediate capsule, and a large main cluster (mITC) located ventro-medial of the basal nucleus. A recent study in mice has identified further subdivisions in these groups of clusters (Busti et al., 2011), and it could be speculated that these groups have different functions. Indeed, cells in the mpITCs and mITC were shown to be activated differentially during high and low fear states, and mpITCs seem to play a critical role during extinction (Likhtik et al., 2008, Busti et al., 2011). Furthermore, cells in the medial cluster (mpITC) are heavily interconnected and constitute a heterogeneous group (Geracitano et al., 2007) comprised of at least three subtypes of projection cells that target 1) mainly other intercalated cells and the mITC, 2) mainly the CeA, 3) project mainly to the amygdala-striatal transition zone (Busti et al., 2011).

Until a few years ago, the canonical view on mpITCs was that they receive inputs from the BLA and the mPFC and inhibit the CeA (Pare et al., 2004). However, the recent discoveries raise the question if we need to rethink how mpITC cell are integrated into fear networks and that they may have more complex inputs and outputs than previously thought. For example, they could receive direct sensory inputs from brain regions that to convey somatosensory information mediating fear learning. Although fiber tracts carrying the sensory afferents (thalamic and cortical) overlap with the location of the mpITC, their innervation and the

functional properties have not been studied. Furthermore, the diversity of mpITC is just beginning to be understood.

Therefore, my PhD project (in Tuebingen) aims at addressing these open questions by assessing the properties, organization, and plasticity of novel inputs to mpITCs and identify the recruited cell-types, using a combination of whole-cell patch clamp recording, two-photon imaging and histological techniques in brain slices of adult mice.

Preliminary findings and aim of the stay

So far, in patch clamp recordings in Tuebingen, I showed that all mpITCs receive monosynaptic, excitatory inputs from external and internal capsule fibers. Tracing experiments confirmed that internal capsule fibers that reach the mpITC originate from the PIN and mGM in the thalamus. When I filled cells during recording and revealed post-hoc I identified different mpITC cell-types based on their projection patterns (similar to the ones previously described in young animals, (Geracitano et al, 2007; Busti et al, 2011). Among these cells, I observed a subset with substantial axonal collaterals in basolateral amygdala. This suggested that this may be a new mpITC cell type with specific targets in the BLA.

Therefore, the aim of my training stay in Innsbruck was learn techniques that would enable me to investigate if I indeed discovered a new mpITC cell type. This requires several steps. 1) to learn to further characterize these cells and their postsynaptic targets using immunofluorescence. 2) to convert fluorescence preparations into permanent DAB preparations and do 2- and 3- dimensional reconstruction of neurons for quantitative analysis, and 3) to learn electron microscopy to confirm that filled axons indeed make synapses and to identify the postsynaptic targets of the putative new cell-type.

Materials and methods

Preparation of slices after biocytin fills

After recording, brain slices were fixed and resectioned at 60 – 70 µm thickness using a vibratome (Microm, Germany). To confirm that cells were filled successfully, I revealed the biocytin-filled mpITC with streptavidin-Cy3. Successfully filled neurons were shipped to Innsbruck for further processing.

Immunofluorescence

To identify the postsynaptic target of a BLA-projecting cell, principal neurons used an immunoreaction against CaMKIIα. Free-floating sections were blocked in 20% normal goat serum (NGS, Vector laboratories), 0.1 % Triton-X100 (TX), in 0.1 M PB for 1h, 30 mins at room temperature. To prevent endogenous antigen recognition, blocking was done with mouse on mouse vector kit (1:30, in PBS) for 20 mins. Sections were then incubated in mouse anti-CaMKIIα (Chemicon, 1:100 in 0.1 M PB, 2 % NGS) at 4˚C, overnight. After extensive washing in 0.1 M PB, sections were incubated in Alexa-350 anti mouse secondary antibody (1: 1000, 0.1 % TX; 2 % NGS in PBS) overnight at 4˚C.

Documentation of cell types and immunostaining

The position of the soma as well as dendritic and axonal arborizations of biocytin-filled mpITC cells were evaluated and documented using using a Carl Zeiss Axioimager M1 microscope equipped with epifluorescence illumination. Images were acquired through a Hamamatsu ORCA-ER CCD camera (Hamamatsu) and analyzed and displayed using the Openlab software (Improvision). The same procedure was followed for documentation of CaMKIIa positive cells and BLA interneurons together with axonal arbors of the streptavidin-Cy3 revealed, biocytin-filled cells in the BLA.

Diaminobenzidine (DAB) convertion and cell reconstruction

Sections from 19 cells were converted with DAB reaction to obtain permanent samples for reconstruction. Sections were washed extensively in 0.1 M PB and then incubated with an avidin-biotin complex (ABC Elite kit, Vector Laboratories) [2 drops of A, 2 drops of B in 5 ml 0.1 M PB containing 1 % BSA, 0.1 % TX] and were visualised with glucose oxidase reaction

(20 % D-glucose, 0.4 % ammonium chloride, 1 % Nickel ammonium sulphate, 0.1 % DAB in 0.1 M PB) using Ni-DAB product as a chromogen.

Camera lucida reconstruction of mpITC cells was performed using a drawing tube mounted onto a Carl Zeiss Axioplan2 microscope with a 40 X, 0.8 NA objective. Drawn sections were merged, scanned and imported into Photoshop (Adobe) for alignment with axonal processes, somatodendritic domains and amygdala nuclear borders in the tissue.

Pre-embedding electron microscopy

Sections from a BLA projecting cell were cryoprotected with 20% w/v sucrose in 0.1 M PB and freeze–thawed over liquid nitrogen to enhance penetration of reagents. The sections containing axon of interest were washed extensively in 0.1 M PB and then incubated with an avidin-biotin complex (ABC Elite kit, Vector Laboratories) [2 drops of A, 2 drops of B in 5 ml 0.1 M PB containing 1 % BSA] and were visualised with glucose oxidase reaction (20 % D-glucose, 0.4 % ammonium chloride, 0.5 % Nickel ammonium sulphate, 0.1 % DAB in 0.1 M PB) using Ni-DAB product as a chromogen. To identify putative postsynaptic target in the BLA, principal neurons were identified with an immunoperoxidase method against CaMKIIα. Free-floating sections were blocked in 20% normal goat serum (NGS, Vector laboratories), 0.05 % TX, in 0.1 M PB for 1h, 30 min at room temperature, incubated at 4˚C for 2 days in 1:100 mouse anti-CaMKIIα in 0.1 M PB, NGS. Sections were washed extensively and incubated overnight at 4˚C with a HRP-coupled goat anti-mouse antibody (Dako) diluted 1:100 in PB 0.1 M, 2% NGS, 0.05 % TX. After washing in 0.1 M PB, sections were incubated in ABC for 1 hr. and revealed using non-intensified DAB (0.05 % DAB in TB, 0.003 % H_2O_2). Contrast was enhanced using 2% osmium tetroxide v/v (Agar Scientific) in 0.1 M PB for 40 min at RT and 1% uranyl acetate w/v (Agar Scientific) in 50% ethanol for 30 min at RT. The sections were dehydrated in increasing gradients of ethanol, immersed in propylene oxide, and embedded in epoxy resin (Durcupan ACM; Sigma-Aldrich) on greased glass slides. Regions of interest containing the axon were dissected under a stereomicroscope and re-embedded in Durcupan ACM. Serial ultrathin sections (70 nm) were cut with an ultramicrotome (Ultracut S; Leica Microsystems) and collected on Formvar-coated copper slot grids. The ultrastructural analysis of the specimens was performed using a Philips CM 120 electron microscope equipped with a Morada CCD TEM camera (Soft Imaging Systems).

Results

Fluorescence documentation, DAB conversion and reconstruction of cells

In order to delineate the projection patterns of different mpTC cells, fluorescence converted biocytin-filled cells were imaged and the extent of axonal projections was evaluated as described above. All documented cells were confirmed to be mpITC cells, as their somata were located within the cluster. Cells were subsequently categorized based on axonal contribution to different nuclei within and outside of the amygdala. I found mpITC cells with 6 different projection patterns. Three of these types have been previously reported in young mice: (Gerracitano et al., 2007, Busti et al., 2011). These include (1) lmC - mITC-projecting cells (Figure 1), which send axons along the lmC to mITC, (2) IPAC/AStr-projecting (Figure 2), which sends axons along the border of the CEA to the amygdala - striatal transition zone and interstitial nucleus of the posterior limb of the anterior commissure, and (3) CEA-projecting cells (Figure 3), which mainly send their axon to the CEA. Four cells representing these three cell-types were converted to light-stable specimens using Ni-DAB product. The somatodendritic tree and axonal arborization were subsequently reconstructed in 2-D using cameralucida as described above.

Among the novel observations are two cells with long-range projections; a caudate putamen (CPu)-projecting cell (Figure 4), which sends axons rostrally to the CPu and a fimbria / internal capsule (Fi/IC)-projecting cell (Figure 5), which sends axon along the internal capsule towards the fimbria. The third novel observation are cells which sends axon collaterals back into the input station of the amygdala, the basolateral nuclei. (BLA-projecting, Figure 6). These cells were observed in 15 % of filled neurons and may constitute a new cell type.

Postsynaptic target identification of BLA-projection cells

In order to identify the postsynaptic targets of BLA-projecting cells, I immunoreacted sections of interest against CamKIIα to labeled principal cells, whereas interneurons were visualized using GAD 67-GFP expression. I observed that the labelled axon appears not to target GAD67- or CaMKIIα-positive somata (Figure 6). This was confirmed in another BLA-projecting cell by electron microscopy in which the axonal terminal in the lateral part of the BLA makes a symmetrical synapse with a dendrite of a cell (Figure 7).

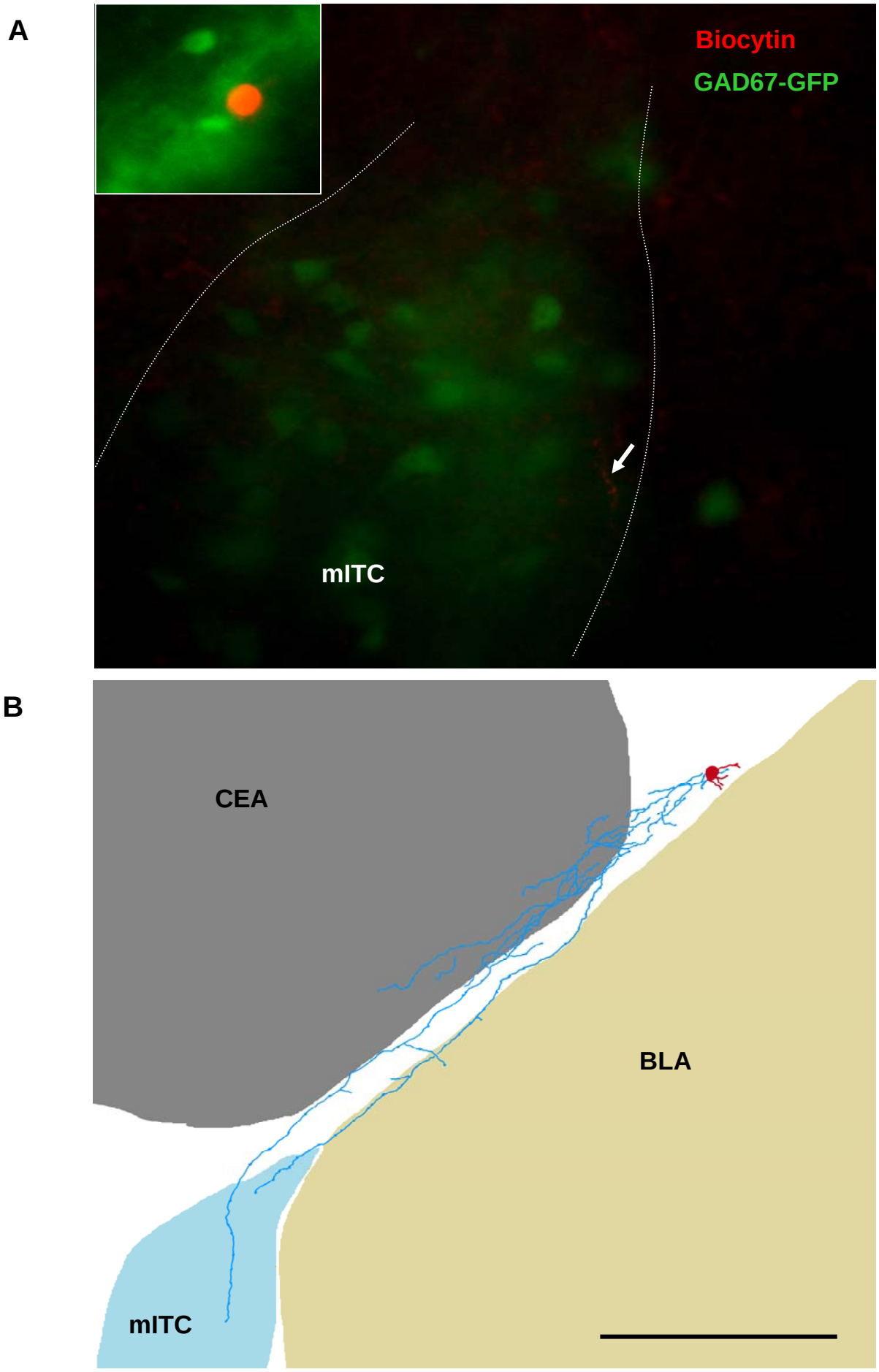

Figure 1. IMC-mITC-projecting cell. (A) Fluorescence micrograph of a mITC-innervating axon (arrow). Inset, high mag. showing the soma within the mpITC (B) Two dimensional reconstruction of the same cell using camera-lucida. Axon in blue, soma and dendrites in red. Abbreviations: BLA basolateral amygdala, CEA central amygdala, mITC main intercalated cell cluster.

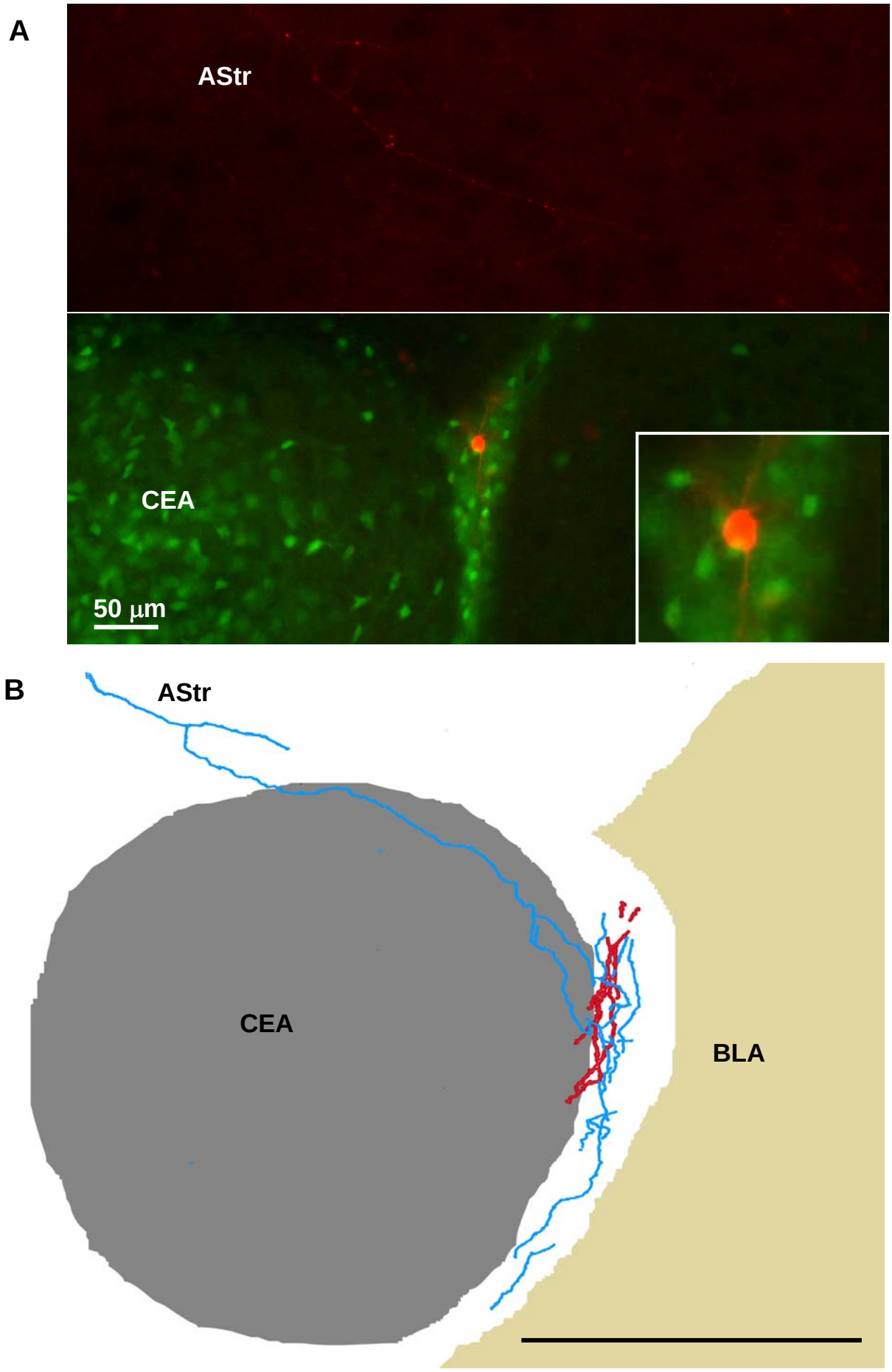

Figure 2. IPAC/AStr-projecting cell. (A) Fluorescence micrographs showing the axon traversing to AStr/IPAC (top) and location of the soma (detail in inset). (B) Two dimensional reconstruction of the same cell using camera-lucida. Axon in blue, soma and dendrites in red.
AStr amygdaloid striatal transition zone, other abbreviations as before.

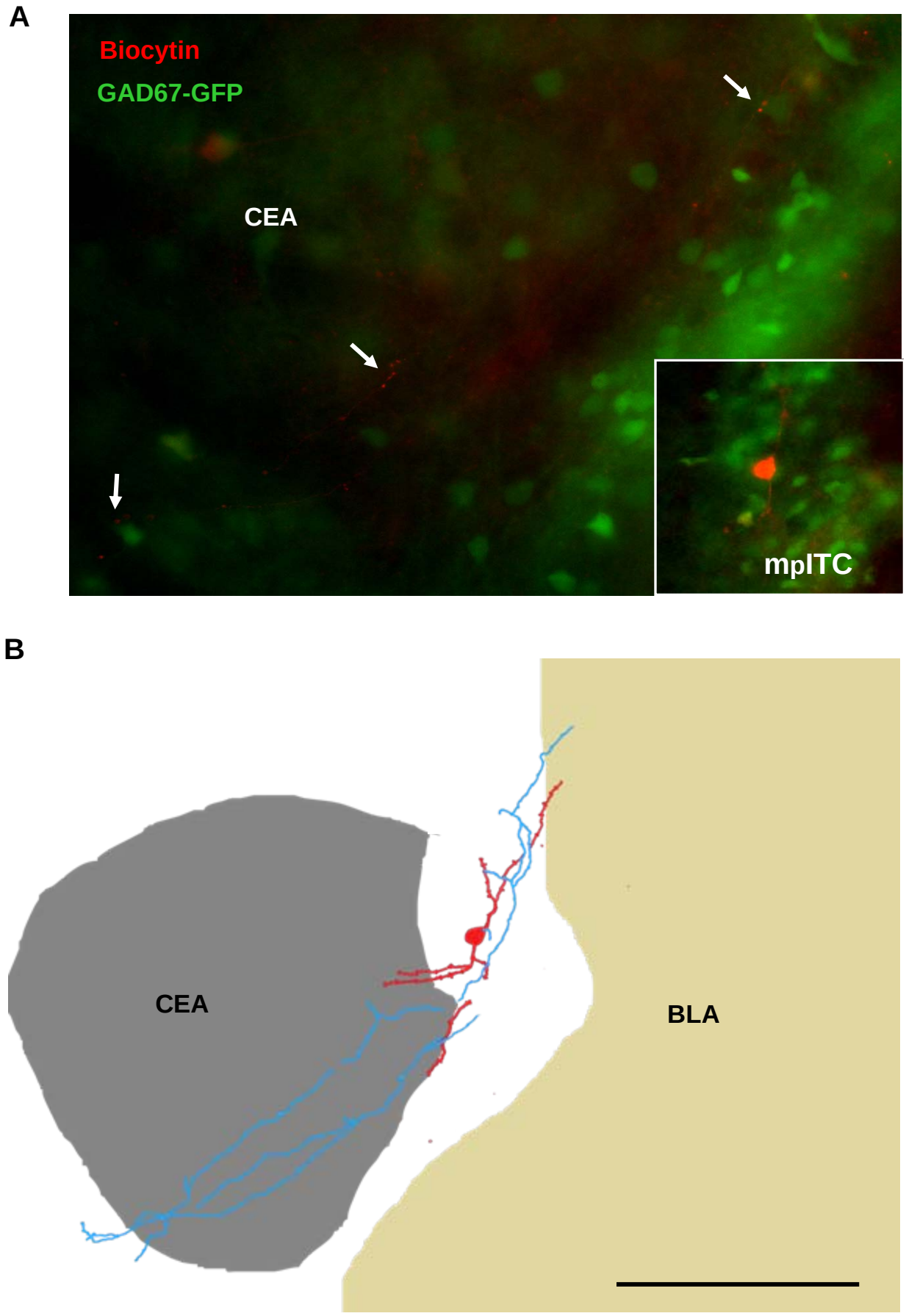

Figure 3. CEA-projecting cell. (A) fluorescence micrograph of a CEA-innervating axon. (B) two-dimensional reconstruction of the same cell using camera-lucida. Axon in blue, soma and dendrites in red. Abbreviations as before.

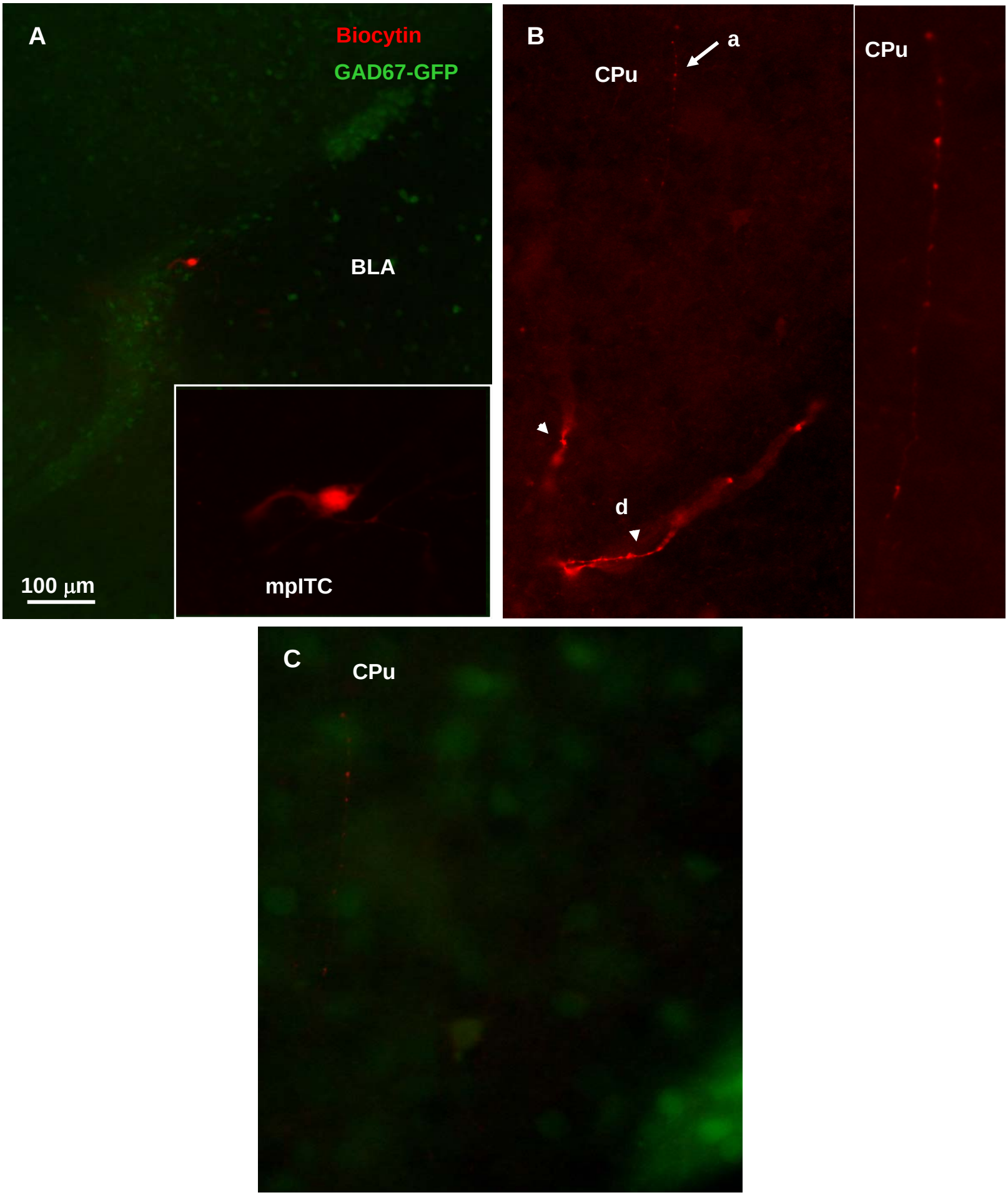

Figure 4. An ITC with long projections to Caudate-Putamen (CPu). (A) fluorescence micrographs showing the soma within mpITC cluster. Inset: higher magnification of soma. (B) Arrowheads indicate dendrites (d), arrow indicates the axon (a) projecting rostrally into CPu. Inset: higher magnification of axon. (C) Another part of the axon projecting to the CPu.

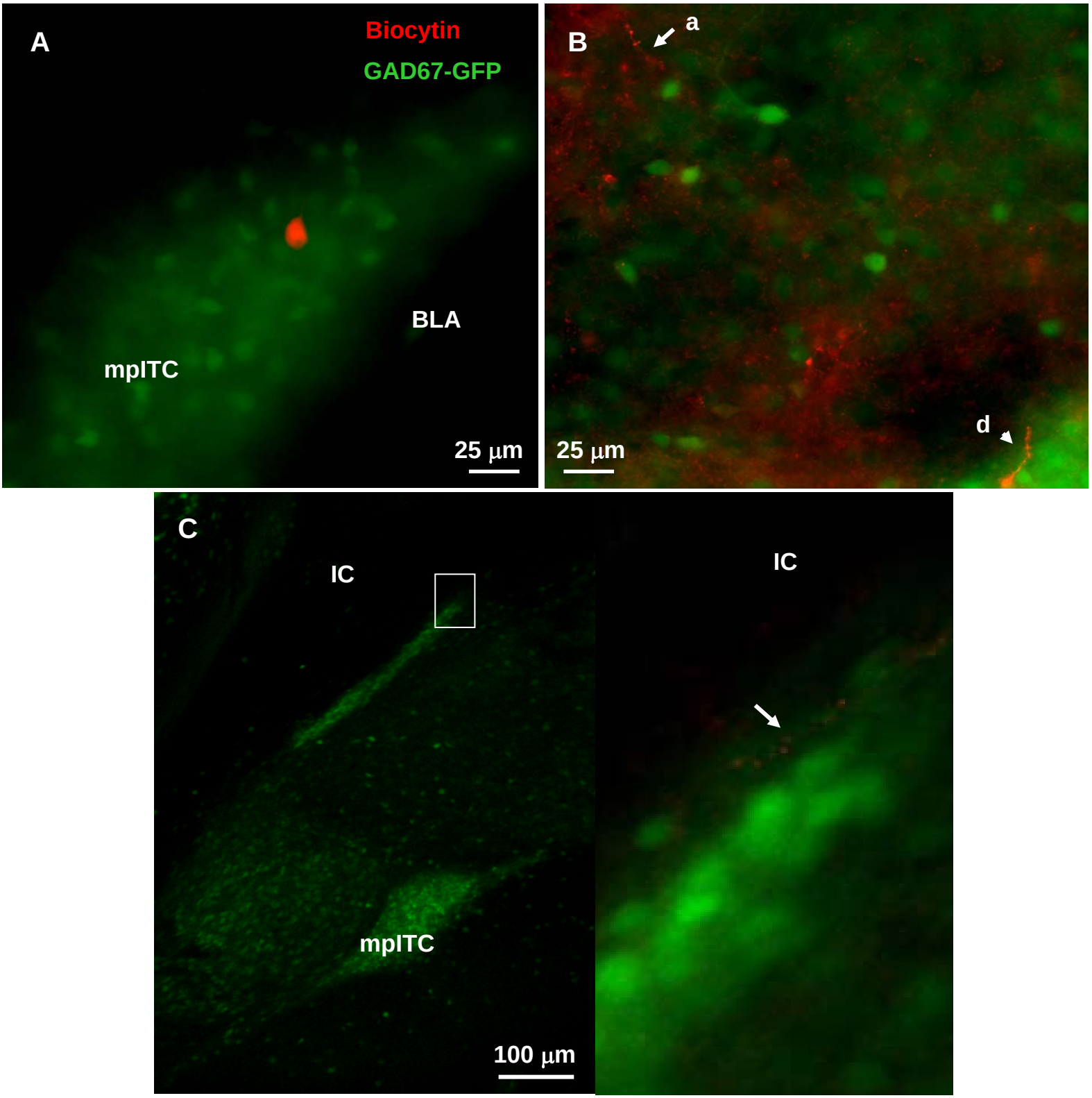

Figure 5. An ITC with long range projections to Fimbria/internal capsule (Fi/IC). (A) Fluorescence micrograph showing the soma of the cell in mpITC cluster. (B) Arrowhead indicates a dendrite (d), arrow indicates the axon (a) tranversing rostro-medially towards IC. (C) Left: lower magnification of position of the IC. Right: higher magnification of the highlighted region showing the axon with varicosities (arrow).

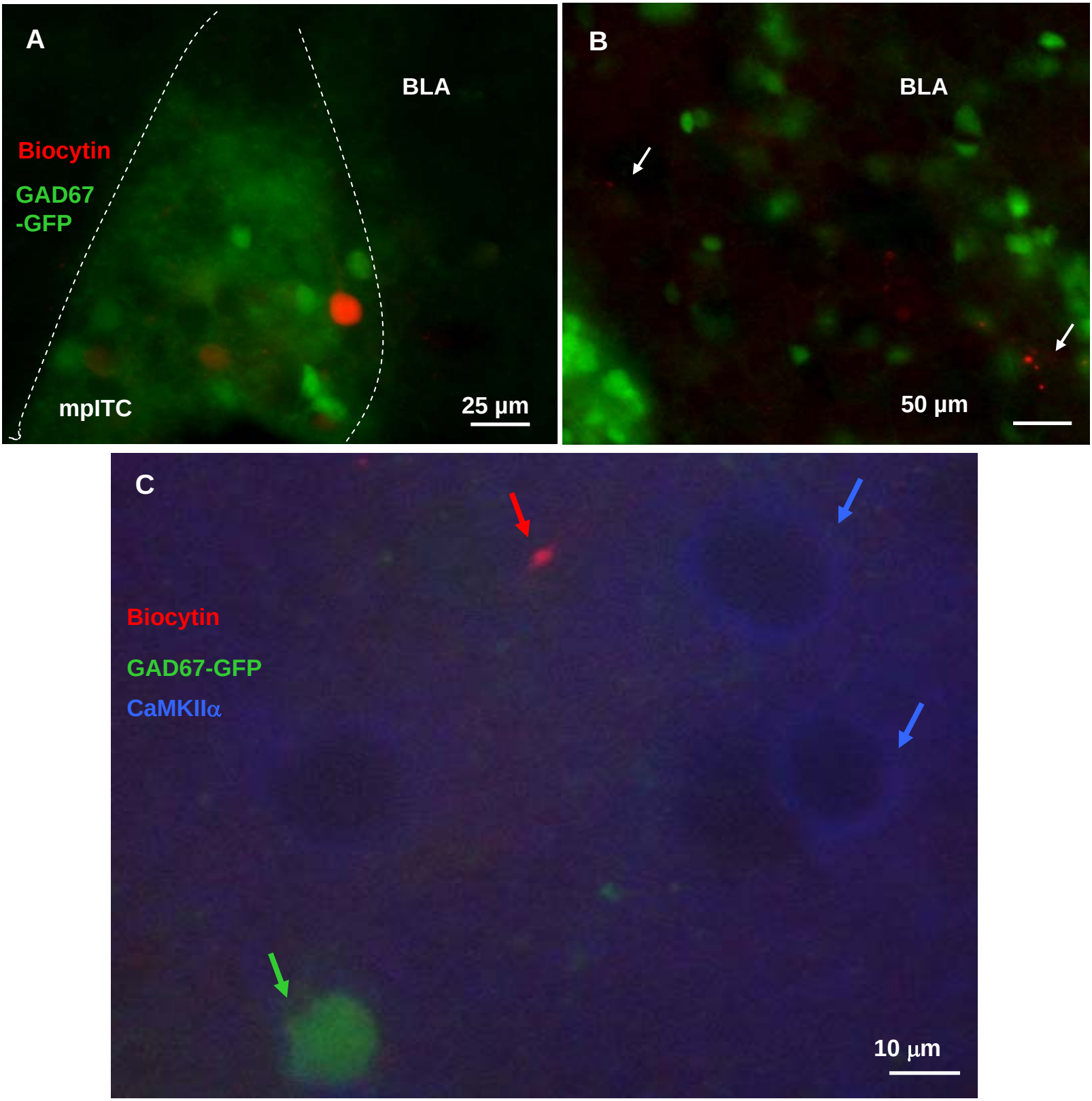

Figure 6. A putative new cell-type: BLA-projecting. (A) fluorescence micrograph showing the soma within the mpITC cluster. (B) Axon of this cell in the BLA. Arrows indicate axonal varicosities. (C) The Axon (red) appears not to target GAD67- (green) or CaMKIIα- (blue) positive somata.

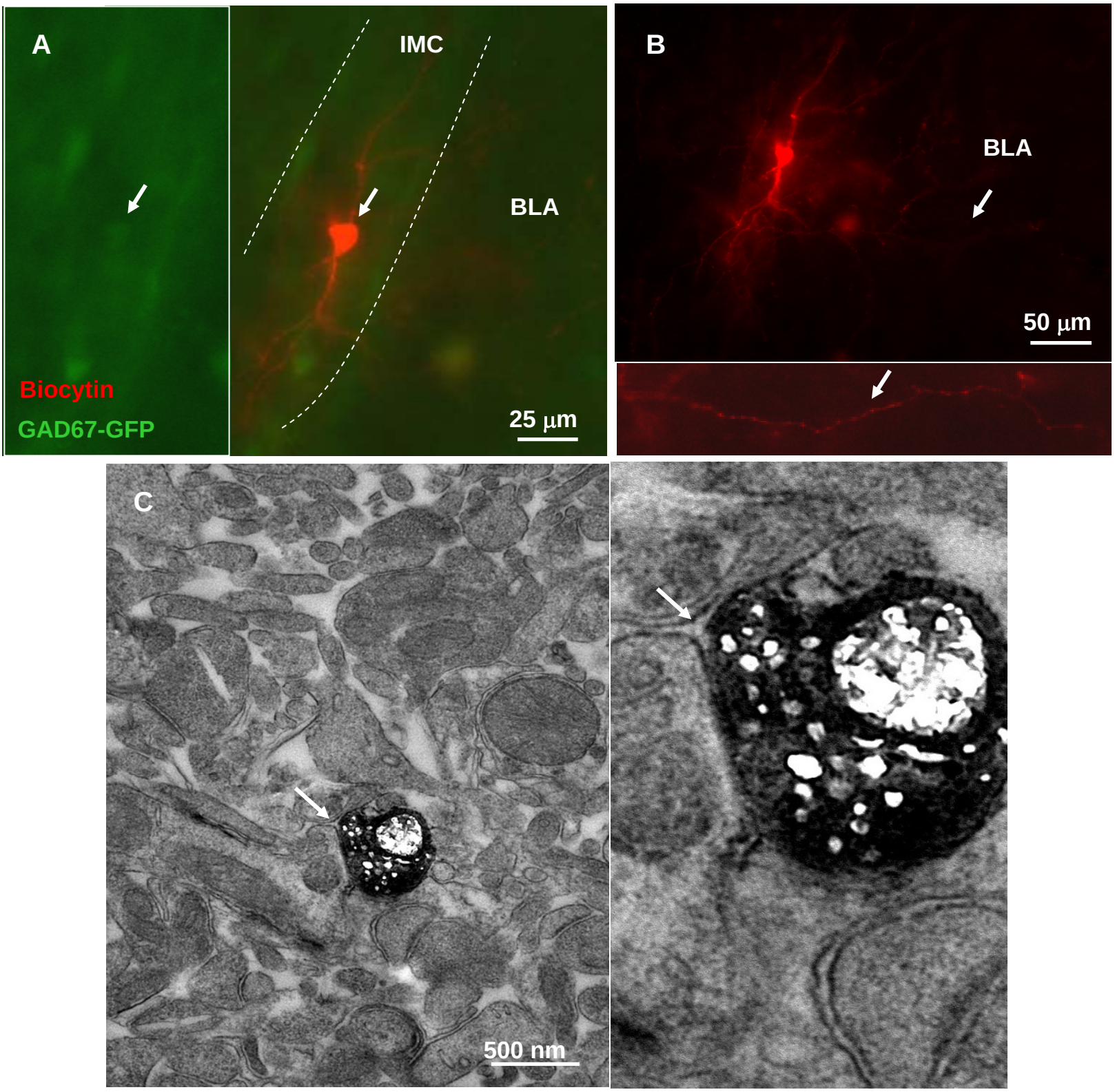

Figure 7. A BLA-projecting cell makes symmetrical synapses in the BLA. (A) fluorescence micrographs showing the soma in red. Left (arrow): the cell is GAD-67 positive. (B) axon of the cell in the BLA. Bottom: higher magnification of the axon. (C) The filled axon (dark) makes a symmetrical synapse with a dendrite of a BLA cell. Note the oval vesicles inside the axon.

Summary

During my stay in Innsbruck, I used epifluorescence microscope to characterize and document different mpITC cell-types. I converted and reconstructed some of them in 2-D using cameralucida. I also learned the basis of 3-D reconstruction using neurolucida. In addition, I learnt to prepare samples for electron microscopy and could confirm that labeled axons make dendritic synapses in the BLA.

Acknowledgements

I thank the NENS for awarding me the stipend for my training stay, without which none of this would have been possible. I would also like to thank my supervisors, Dr Ingrid Ehrlich (home institute) and Professor Francesco Ferraguti (host institute) for giving me this opportunity.
Special thanks to Gabi Schmidt for teaching me some techniques, and the all members of Prof. Ferraguti's lab for making my stay a memorable one.

References

Busti D., Geracitano R., Whittle N., Dalezios Y., Manko M., Kaufmann W., Satzler K., Singewald N., Capogna M., Ferraguti F. (2011) Different fear states engage distinct networks within the intercalated cell clusters of the amygdala. J Neurosci 31:5131-5144.

Geracitano R., Kaufmann W.A., Szabo G., Ferraguti F., Capogna M. (2007) Synaptic heterogeneity between mouse paracapsular intercalated neurons of the amygdala. J Physiol 585:117-134.

Killcross S., Robbins T.W., Everitt B.J. (1997) Different types of fear-conditioned behaviour mediated by separate nuclei within amygdala. Nature 388:377-380.

Krettek J.E., Price J.L. (1978) A description of the amygdaloid complex in the rat and cat with observations on intra-amygdaloid axonal connections. J Comp Neurol 178:255-280.

Likhtik E., Popa D., Apergis-Schoute J., Fidacaro G.A., Paré D. (2008) Amygdala intercalated neurons are required for expression of fear extinction. Nature 454:642-645.

McDonald A.J. (1982) Cytoarchitecture of the central amygdaloid nucleus of the rat. J Comp Neurol 208:401-418.

Millhouse O.E. (1986) The intercalated cells of the amygdala. J Comp Neurol 247:246-271.

Pare D., Quirk G.J., Ledoux J.E. (2004) New vistas on amygdala networks in conditioned fear. J Neurophysiol 92:1-9.

Pare D., Smith Y. (1993) The intercalated cell masses project to the central and medial nuclei of the amygdala in cats. Neuroscience 57:1077-1090.

Swanson L.W., Petrovich G.D. (1998) What is the amygdala? Trends Neurosci 21:323-331.